

Supporting Information for

**Towards quantitative and scalable transformation of furfural to cyclopentanone
with supported gold catalysts**

Gao-Shuo Zhang, Ming-Ming Zhu, Qi Zhang, Yong-Mei Liu, He-Yong He, and Yong Cao*

*Department of Chemistry, Shanghai Key Laboratory of Molecular Catalysis and Innovative Materials,
Fudan University, Shanghai 200433, P. R. China*

E-mail: yongcao@fudan.edu.cn

Table S1. Effect of additives on the transformation of furfural (FFA) over 0.73 wt% Au/TiO₂-A.^[a]

Entry	Additive	Conv. [%]	Mass balance [%]	Sel. [%]				
				CPO	CPL	MF	FAL	CEON
1	Na ₂ CO ₃	>99	27±5	0	0	3	24	0
2	Na ₂ HPO ₄	>99	48±3	0	0	7	41	0
3	none	>99	99±1	>99	0	0	0	0
4	NaH ₂ PO ₄	>99	64±3	47	1	0	11	5
5	H ₃ PO ₄	>99	31±5	19	2	0	4	6

[a] Reaction conditions: FFA (5.2 mmol), H₂O (10 mL), additive (0.1 mmol), H₂ (4 MPa), S/C (2000), 160 °C, 1.2 h.

Table S2. The hydrogenation of FFA over platinum-group-metal (PGM)-based catalysts.^[a]

Entry	catalyst ^[b]	Conv. [%]	Mass balance [%]	Sel. [%]				
				CPO	CPL	MF	FAL	CEON
1	Pt/TiO ₂ -A (0.73 wt%)	87	87±3	71	5	11	0	0
2	Pd/TiO ₂ -A (0.73 wt%)	23	95±2	87	1	6	0	1
3	Ir/TiO ₂ -A (0.73 wt%)	56	93±2	34	0	0	0	59
4	Rh/TiO ₂ -A (0.73 wt%)	41	94±2	93	0	0	0	1

[a] Reaction conditions: FFA (5.2 mmol), H₂O (10 mL), H₂ (4 MPa), S/C (2000), 160 °C, 1.2 h.

Table S3. The hydrogenation of FFA over TiO₂-A supported noble catalysts at 80 °C.^[a]

Entry	catalyst	Conv. [%]	Sel. [%]	
			FAL	other
1	Au/TiO ₂ -A (0.73 wt%)	31	99	0
2	Pt/TiO ₂ -A (0.73 wt%)	82	99	0
3	Pd/TiO ₂ -A (0.73 wt%)	63	99	0

[a] Reaction conditions: FFA (5.2 mmol), H₂O (10 mL), H₂ (4 MPa), S/C (2000), 80 °C, 1.2 h.

Table S4. The effect of different-sized gold particles and various gold loadings on the transformation of FFA to CPO.^[a]

Entry	Catalyst	Average particle size [nm]	Conv. [%]	TOF ^[b] [h ⁻¹]	Mass balance [%]	Sel. [%]			
						CPO	CPL	FAL	CEON

1	Au/TiO ₂ -A (0.73wt%)	2.1	>99	7520	99±1	>99	0	0	0
2	Au/TiO ₂ -A (0.71wt%)	4.6 ^[c]	35	680	99±1	36	0	25	38
3	Au/TiO ₂ -A (0.75wt%)	8.4 ^[d]	16	270	99±1	25	0	28	46
4	Au/TiO ₂ -A (0.24wt%)	2.1	>99	7560	99±1	>99	0	0	0
5	Au/TiO ₂ -A (0.10wt%)	2.0	>99	7470	99±1	>99	0	0	0

[a] Reaction conditions: FFA (5.2 mmol), H₂O (10 mL), H₂ (4 MPa), S/C (2000), 160 °C, 1.2 h; [b] TOF values based on total the gold loading at FFA conversion of 15%; [c] Figure S9e; [d] Figure S9f.

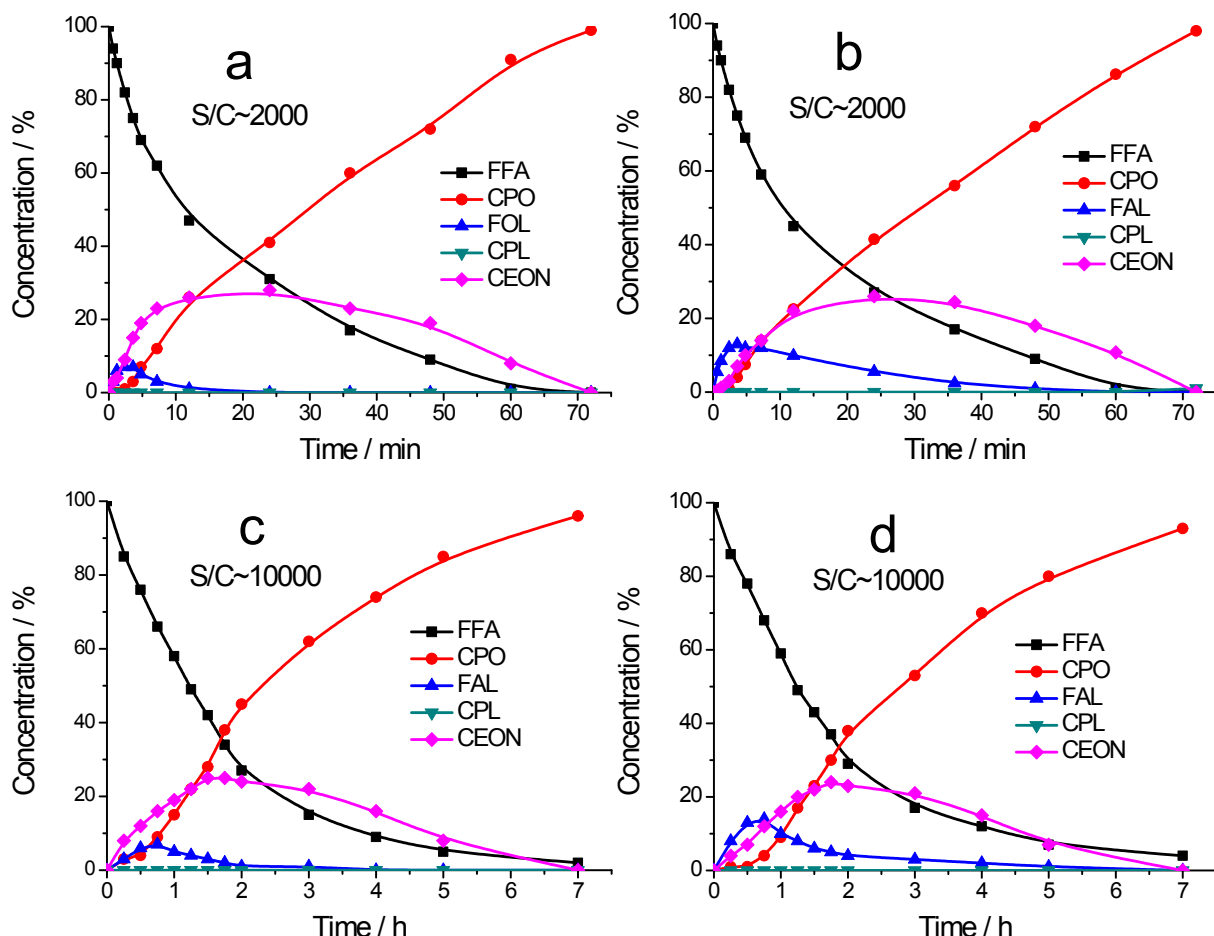
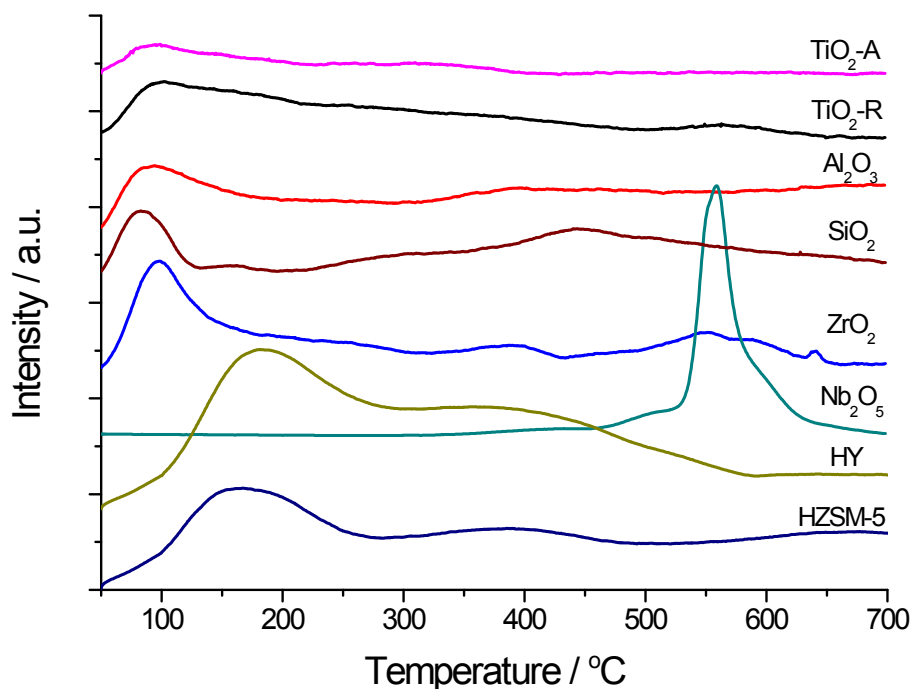


Figure S1. Reaction profiles for the hydrogenation of FFA over a series of Au/TiO₂-A catalysts with different gold loading content or S/C levels. (a) 0.24 wt% Au/TiO₂- A (S/C~2000); (b) 0.73 wt% Au/TiO₂-A mixed with seven-fold bare TiO₂-A (S/C~2000); (c) 0.24 wt% Au/TiO₂-A (S/C~10000); (d) 0.73 wt% Au/TiO₂-A (S/C~10000). Reaction condition: FFA (5.2 mmol), H₂O (10 mL), H₂ (4 MPa), 160 °C.

Table S5. The effect of reaction temperature and hydrgen pressure on the transformation of FFA to CPO over 0.10 wt% Au/TiO₂-A.^[a]

Entry	H ₂ [MPa]	T [°C]	Conv. [%]	Mass balance [%]	Sel. [%]			
					CPO	CPL	FAL	CEON
1	4	120	42	99±1	18	0	71	10
2	4	140	77	99±1	76	0	10	13
3	4	160	>99	99±1	>99	0	0	0
4	4	180	>99	95±2	88	7	0	0
5	3	160	92	99±1	86	0	0	13
6	5	160	>99	99±1	96	3	0	0

[a] Reaction conditions: FFA (5.2 mmol), H₂O (10 mL), S/C (2000), 1.2 h.



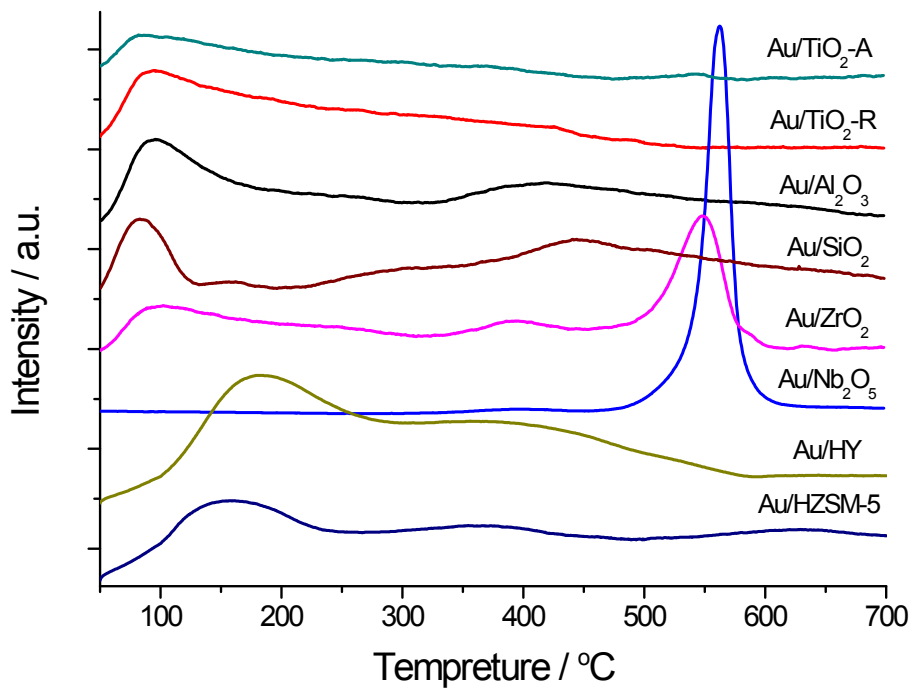


Figure S2. NH_3 -TPD profiles of various supports and gold catalysts.

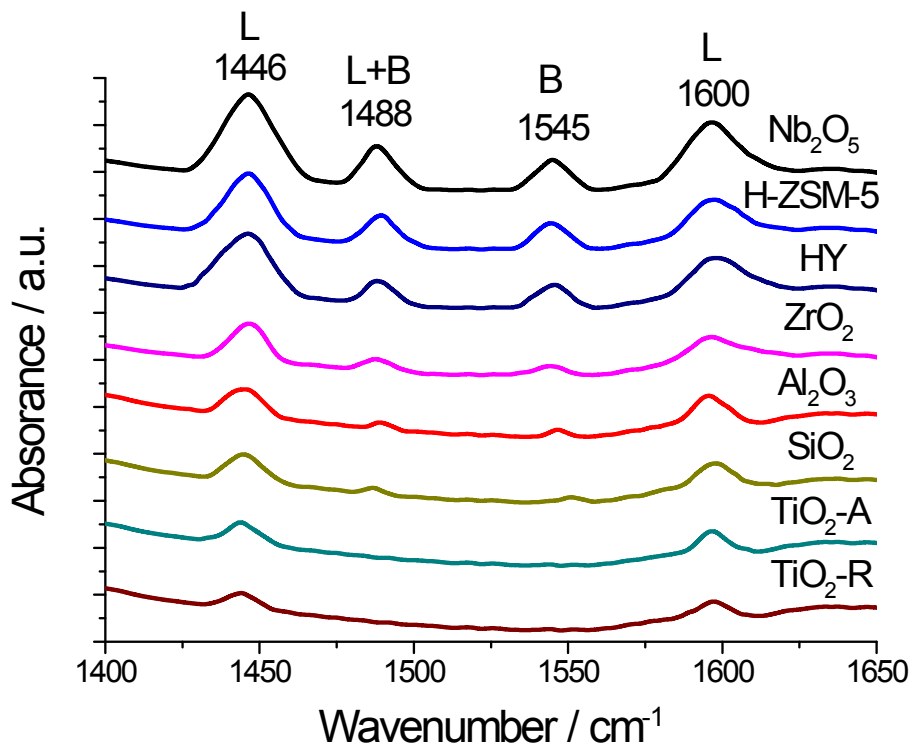
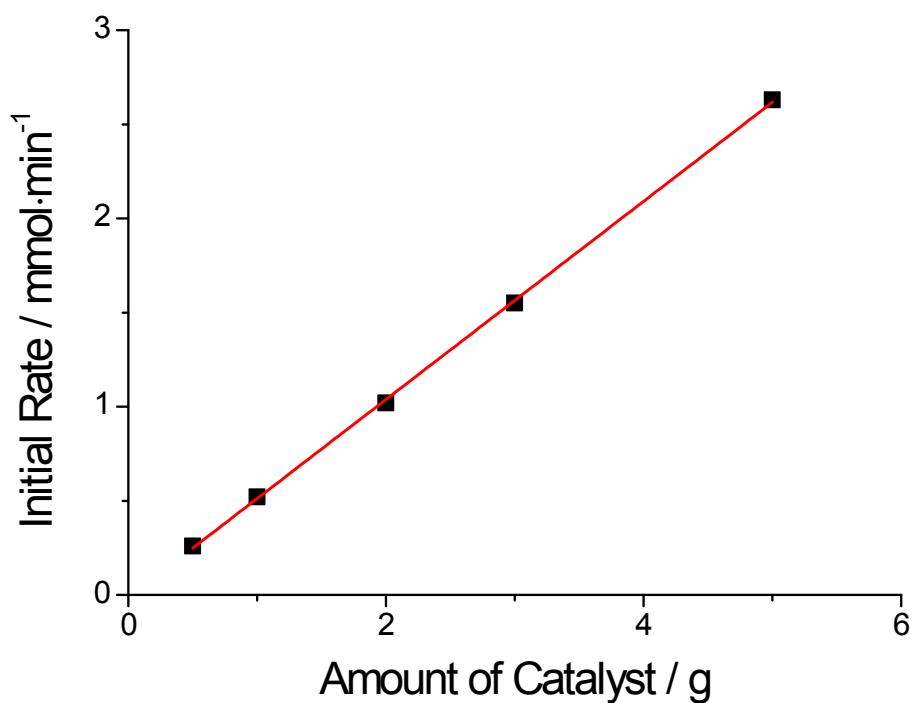
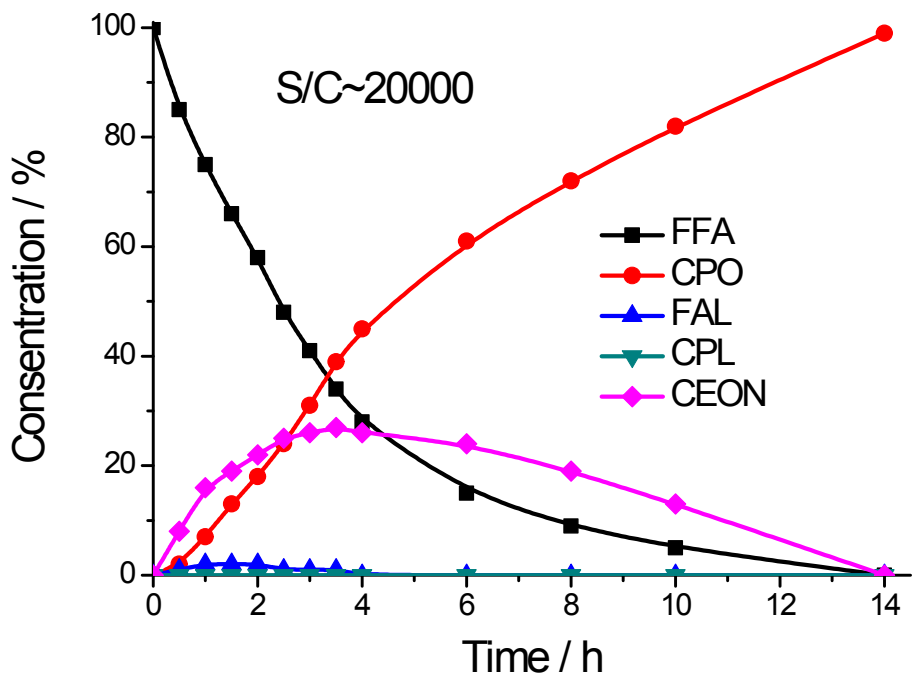


Figure S3. FTIR spectra of pyridine adsorbed onto the various oxide supports.



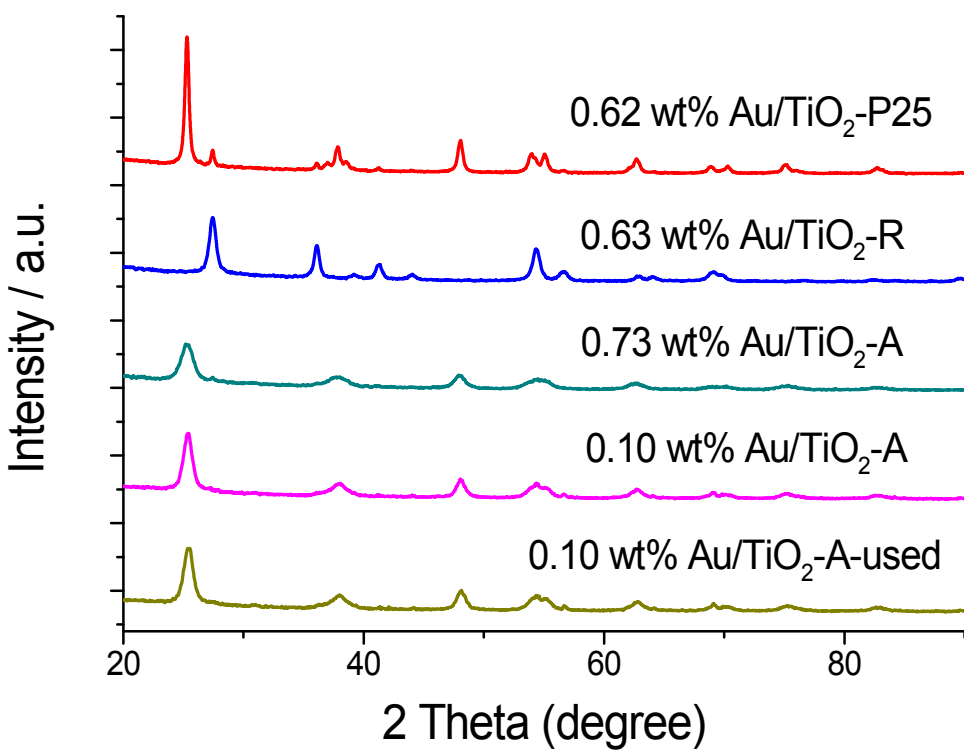


Figure S6. Powder XRD patterns of various Au/TiO₂ catalysts.

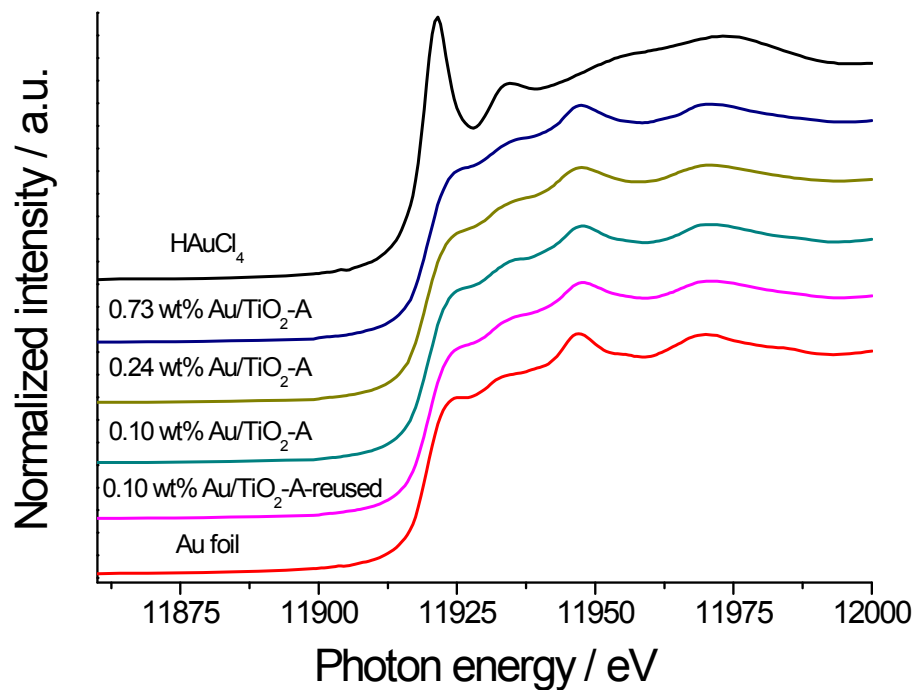
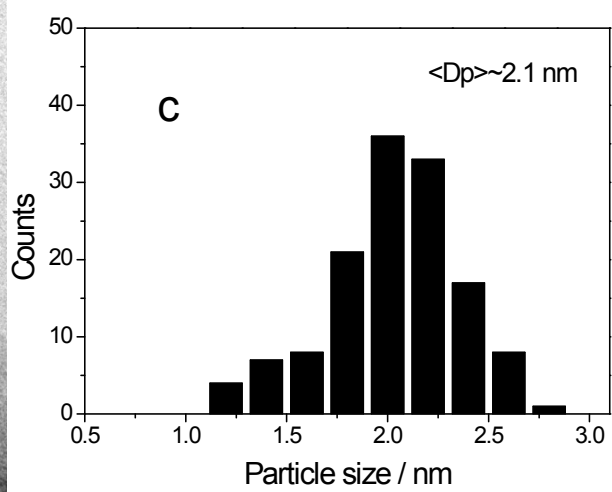
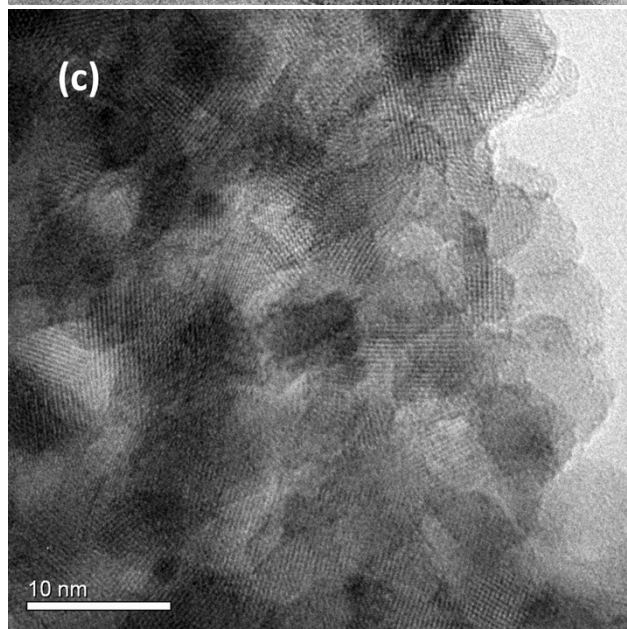
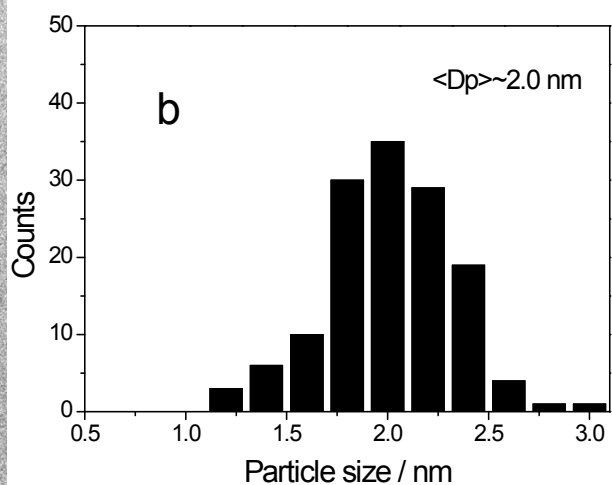
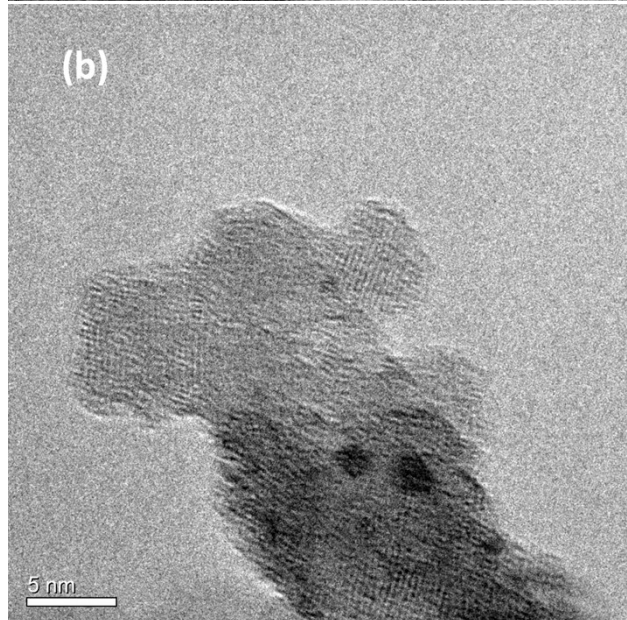
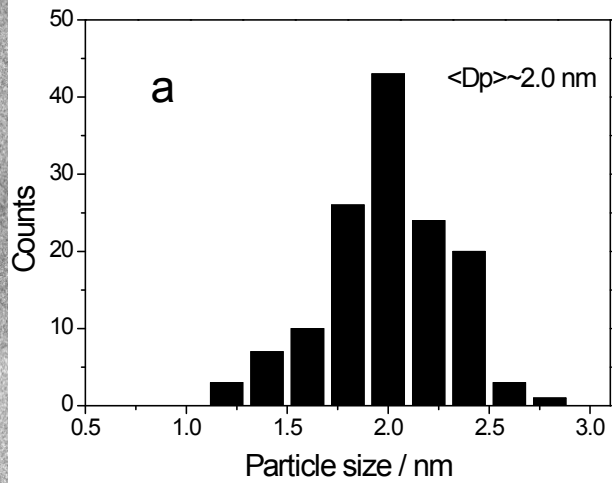
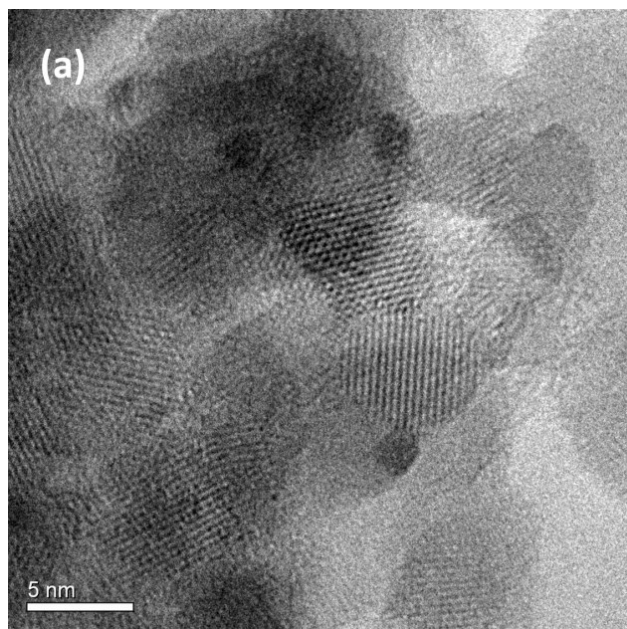
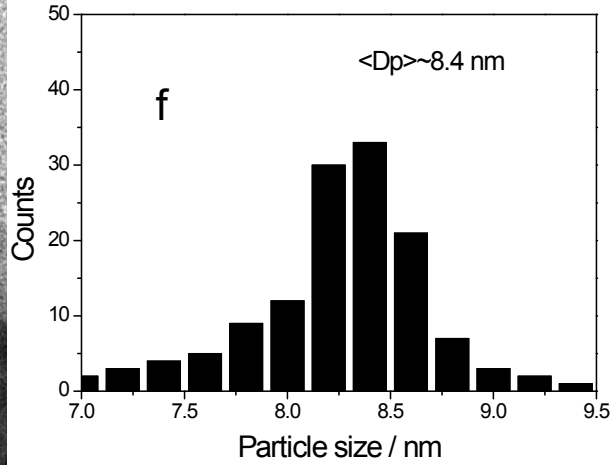
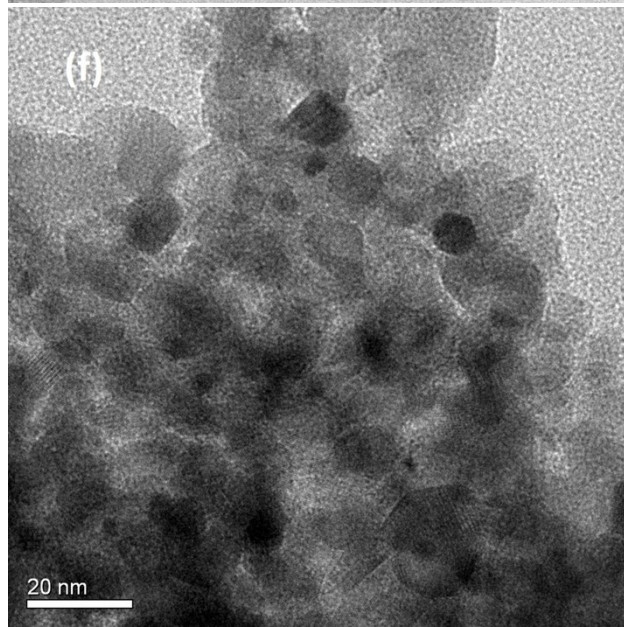
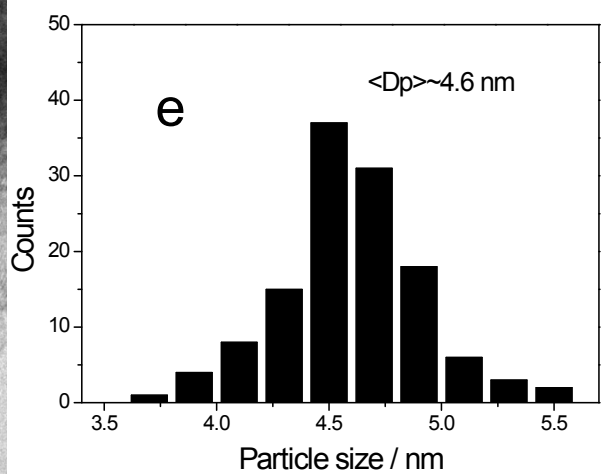
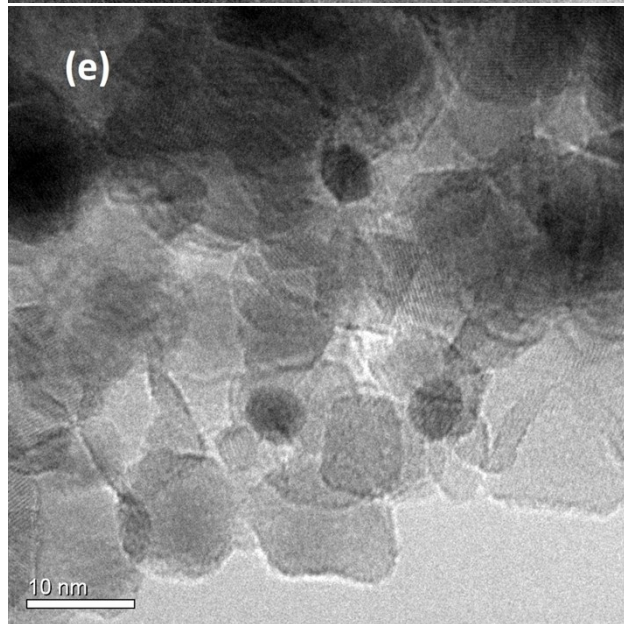
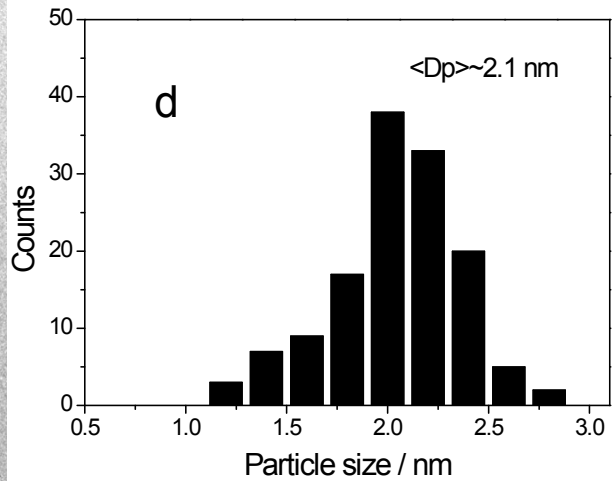
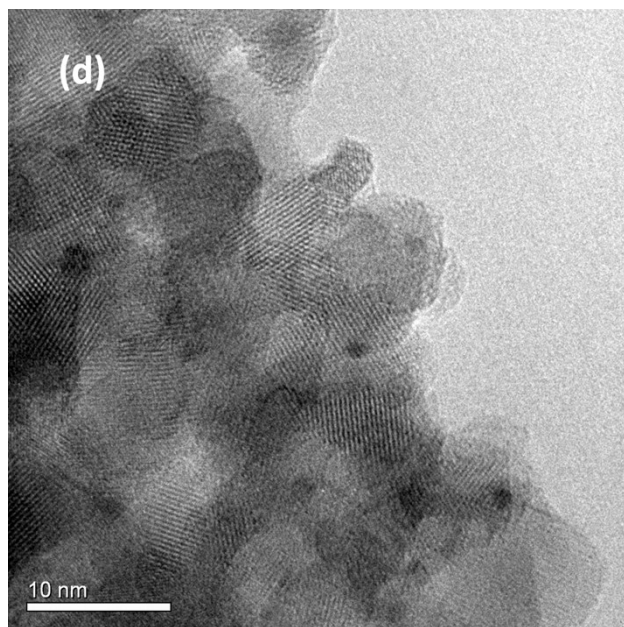
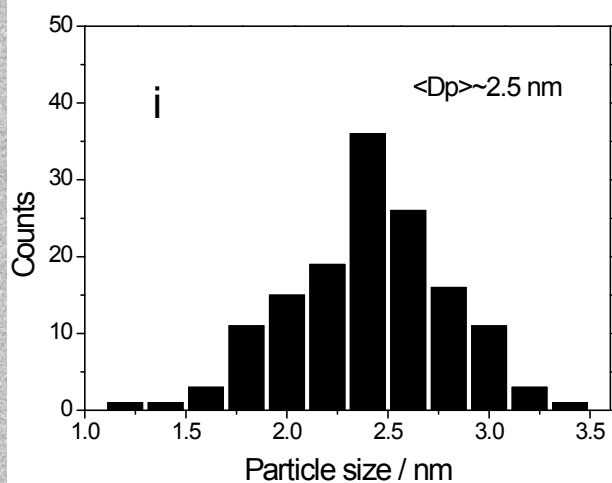
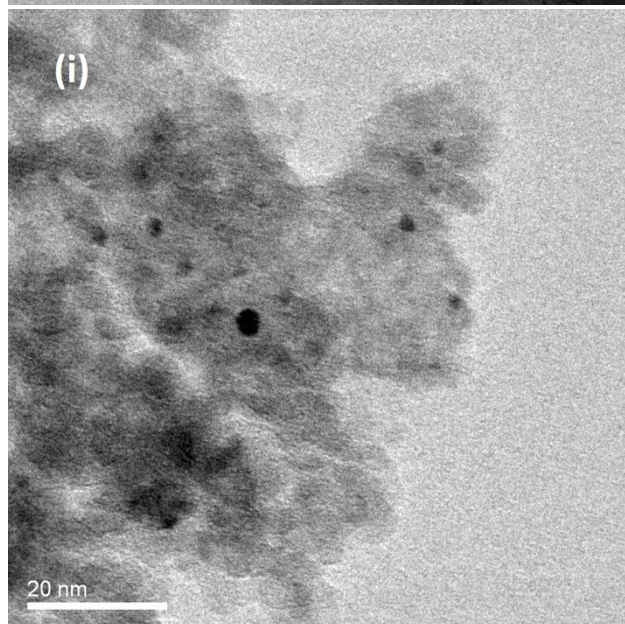
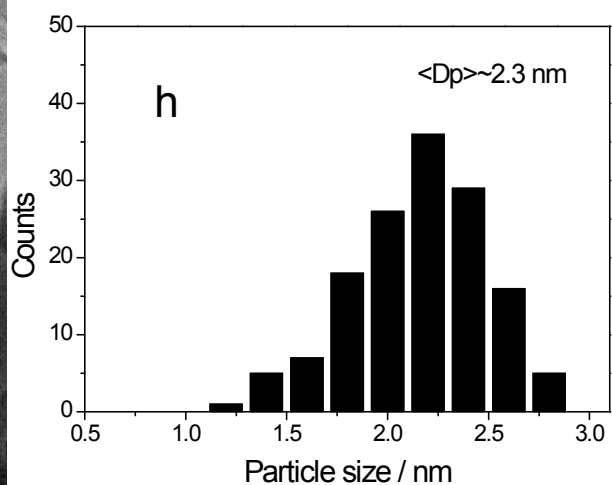
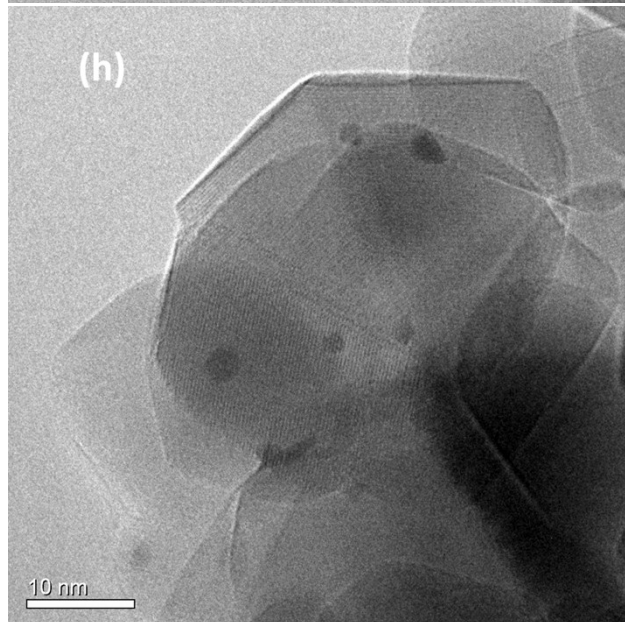
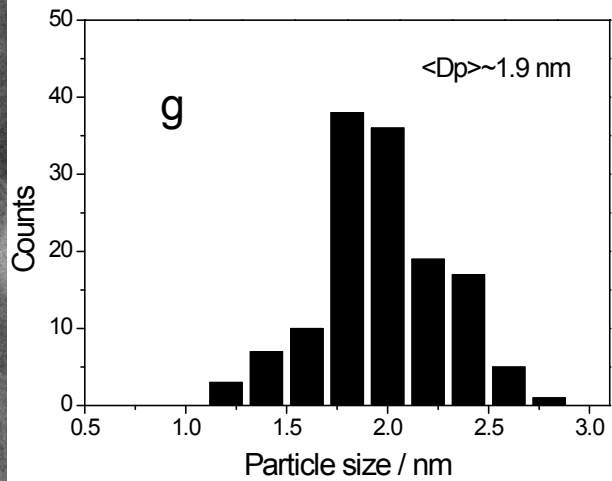
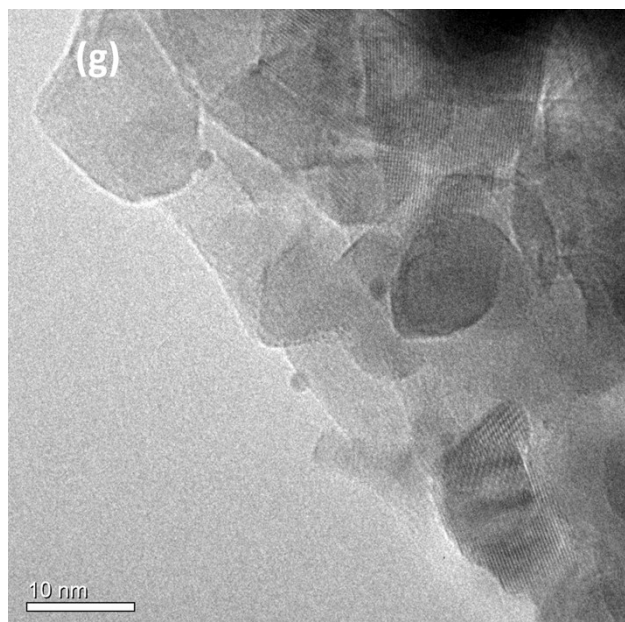
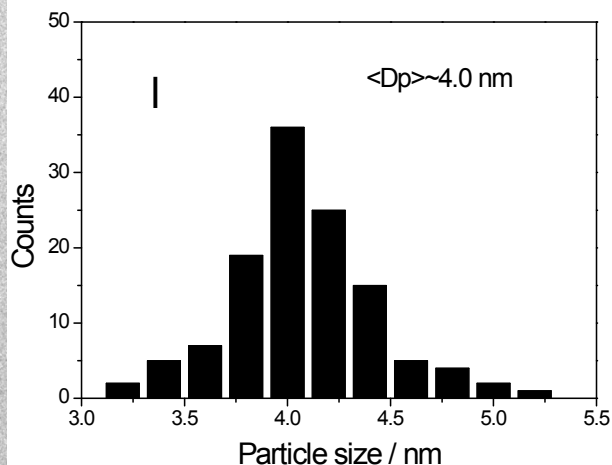
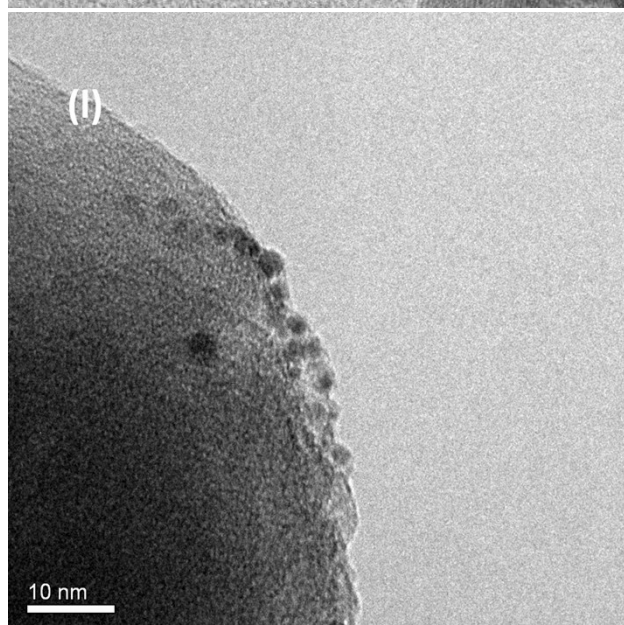
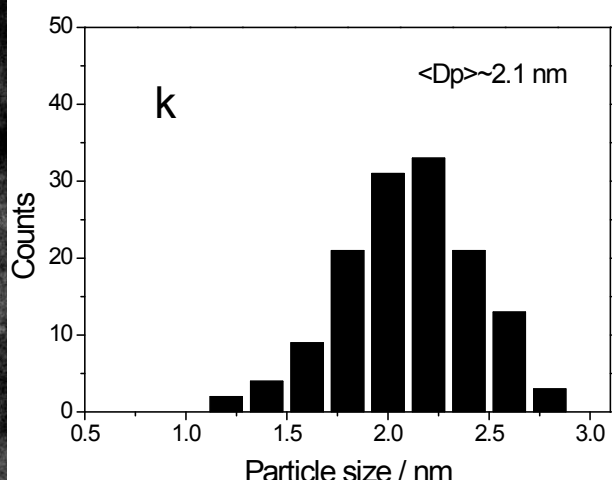
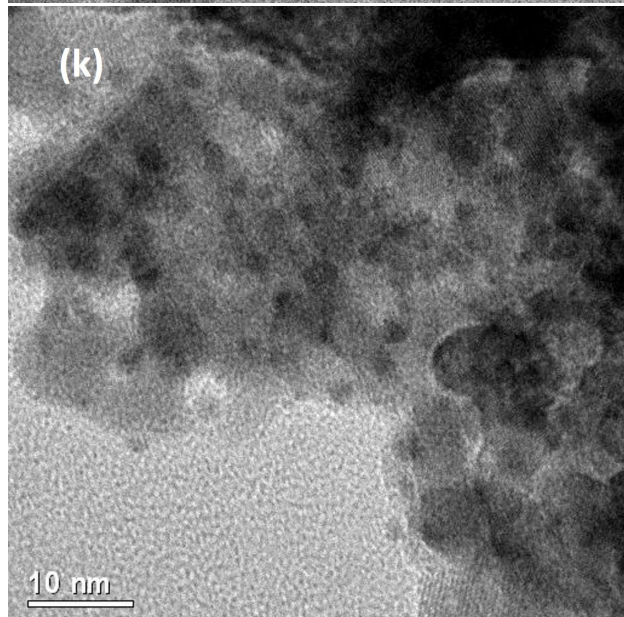
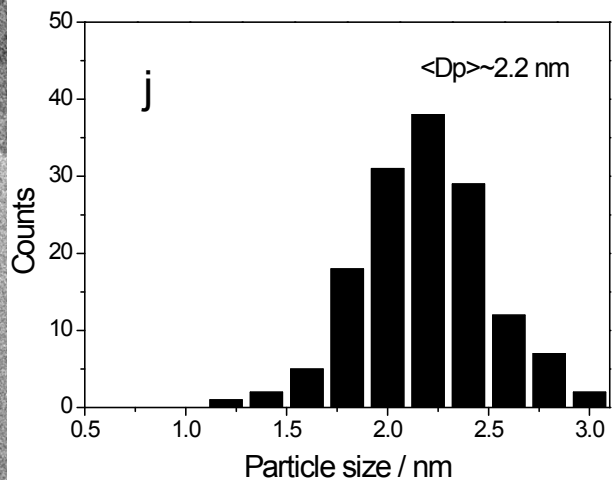
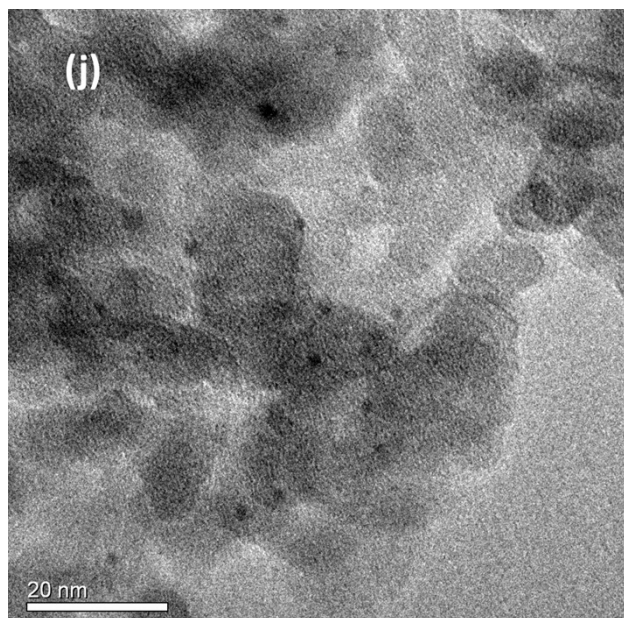


Figure S7. XANES analysis of Au/TiO₂-A catalyst.









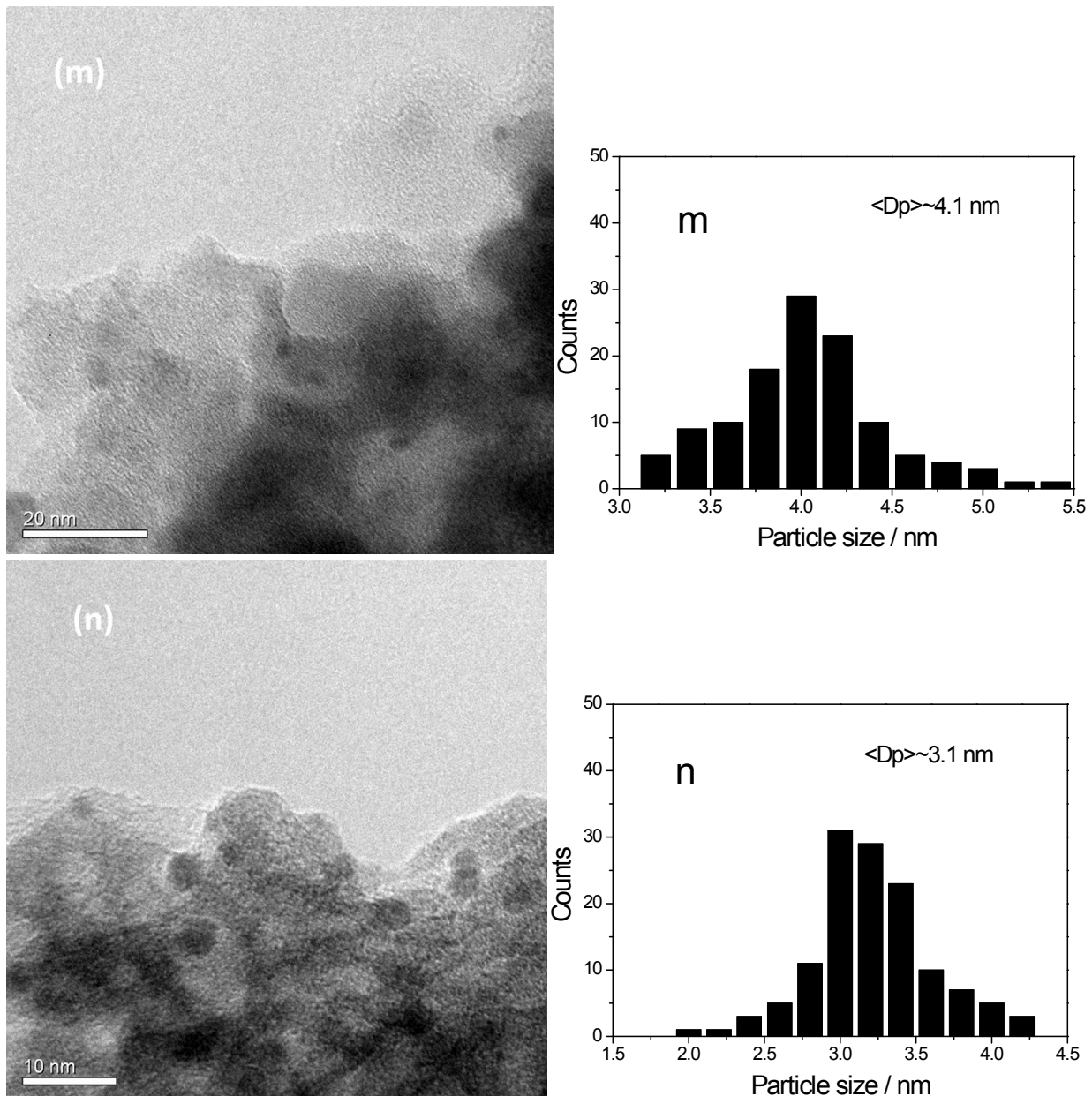


Figure S8. TEM analysis of various catalysts (a) 0.10 wt% Au/TiO₂-A; (b) 0.10 wt% Au/TiO₂-A-reused; (c) 0.24 wt% Au/TiO₂-A; (d) 0.73 wt% Au/TiO₂-A; (e) 0.71 wt% Au/TiO₂-A (4.6 nm); (f) 0.75 wt% Au/TiO₂-A (8.4 nm); (g) 0.63 wt% Au/TiO₂-R; (h) 0.62 wt% Au/TiO₂-P25; (i) 0.85 wt% Au/Al₂O₃; (j) 0.65 wt% Au/SiO₂; (k) 0.68 wt% Au/ZrO₂; (l) 0.64 wt% Au/HY; (m) 0.62 wt% Au/H-ZSM-5; (n) 0.61 wt% Au/Nb₂O₅.

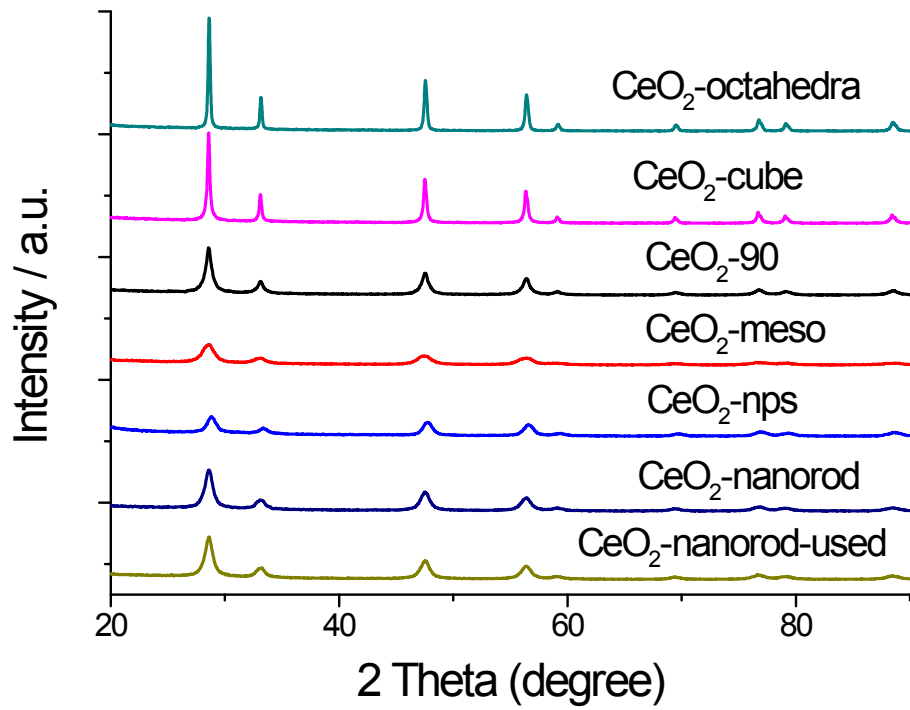
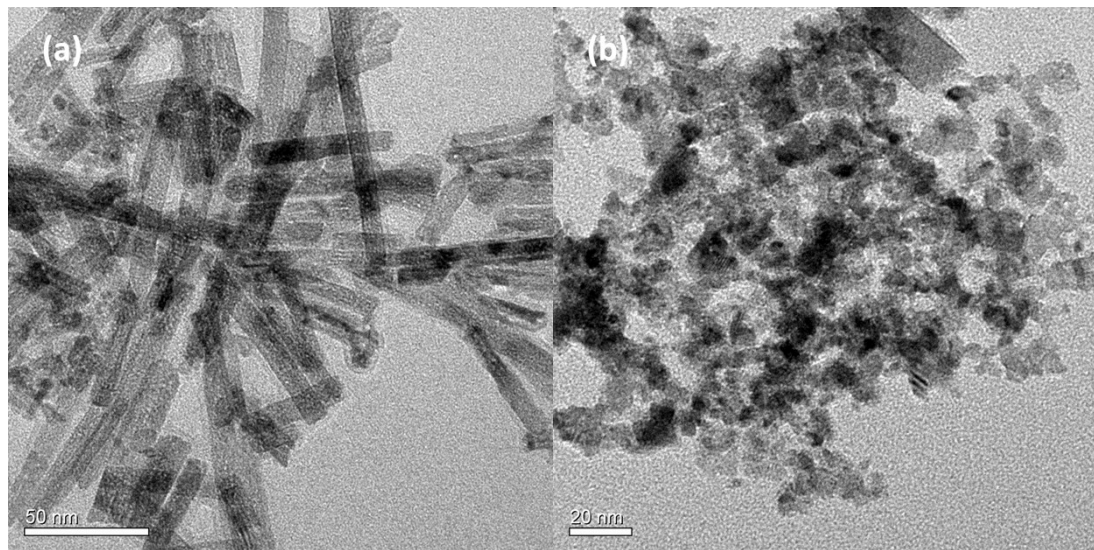


Figure S9. XRD analysis of various forms of nanostructured CeO₂.



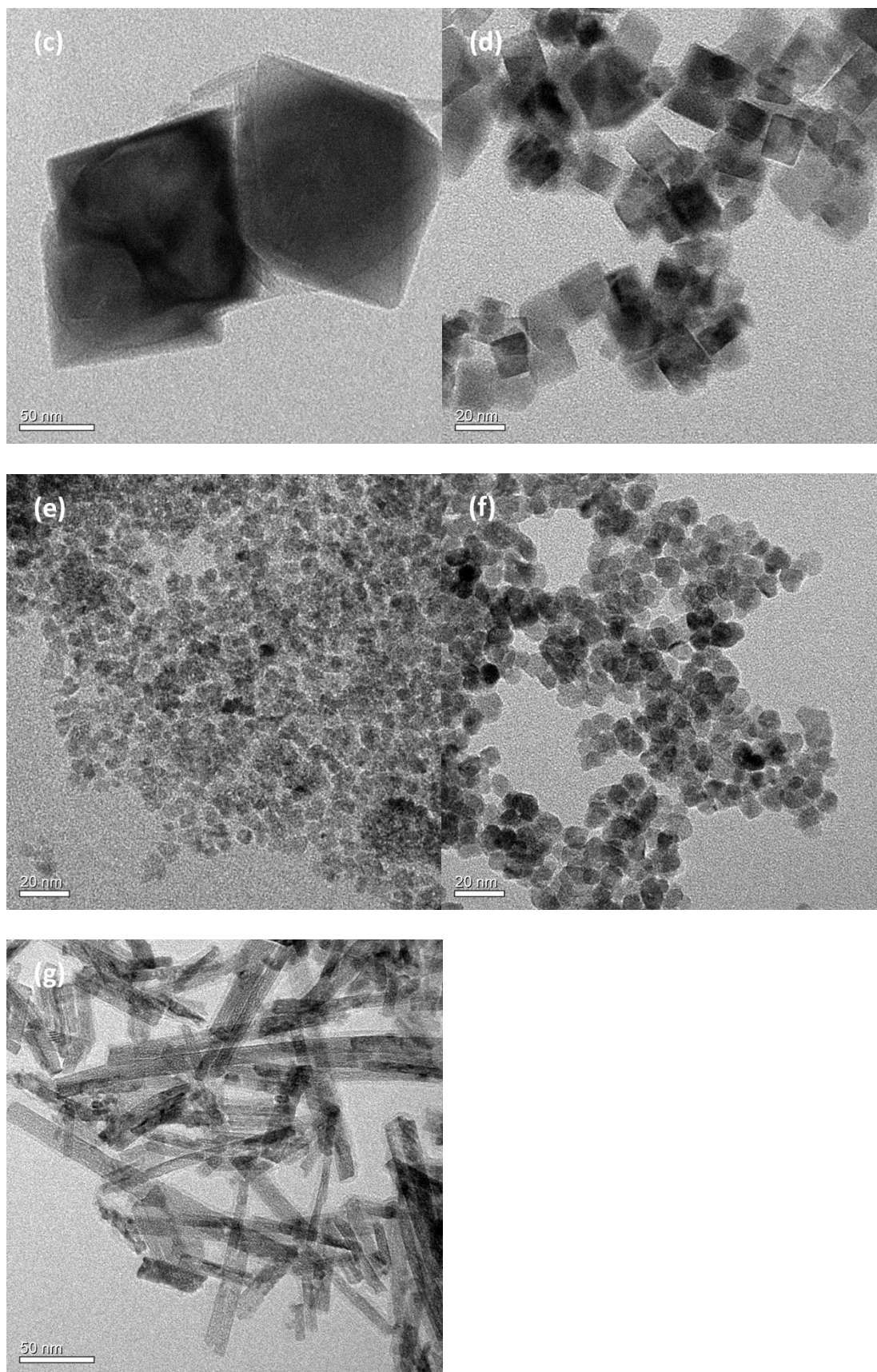


Figure S10. TEM analysis of various forms of nanostructured CeO₂. (a) CeO₂-nanorods; (b) CeO₂-90; (c) CeO₂-octahedra; (d) CeO₂-cube; (e) CeO₂-meso; (f) CeO₂-nps; (g) CeO₂-nanorods-used.